THE JOURNAL OF BIOLOGICAL CHEMISTRY VOL. 283, NO. 42, pp. 28392–28400, October 17, 2008

Phosphorylation of MyoGEF on Thr-574 by Plk1 Promotes MyoGEF Localization to the Central Spindle*[S]

Received for publication, March 6, 2008, and in revised form, August 5, 2008 Published, JBC Papers in Press, August 11, 2008, DOI 10.1074/jbc.M801801200

Michael Asiedu[‡], Di Wu[‡], Fumio Matsumura[§], and Qize Wei[‡1]

From the [‡]Department of Biochemistry, Kansas State University, Manhattan, Kansas 66506 and the [§]Department of Molecular Biology & Biochemistry, Rutgers University, Piscataway, New Jersey 08855

We reported previously that a guanine nucleotide exchange factor, MyoGEF, localizes to the central spindle, activates RhoA, and is required for cytokinesis. In this study, we have found that Plk1 (polo-like kinase 1) can phosphorylate MyoGEF, thereby recruiting MyoGEF to the central spindle as well as enhancing MyoGEF activity toward RhoA. The *in vitro* kinase assay shows that Plk1 can phosphorylate MyoGEF on threonine 574. Immunoprecipitation/immunoblot analysis demonstrates that mutation of threonine 574 to alanine dramatically decreases threonine phosphorylation of MyoGEF in transfected HeLa cells, suggesting that threonine 574 is phosphorylated *in vivo*. Consistent with these observations, immunofluorescence shows that Plk1 and MyoGEF colocalize at the spindle pole and central spindle during mitosis and cytokinesis. Importantly, RNA interference-mediated depletion of Plk1 interferes with the localization of MyoGEF at the spindle pole and central spindle. Moreover, mutation of threonine 574 to alanine in MyoGEF or depletion of Plk1 by RNA interference leads to a decrease in MyoGEF activity toward RhoA in HeLa cells. Therefore, our results suggest that Plk1 can regulate MyoGEF activity and localization, contributing to the regulation of cytokinesis.

Plk1 (polo-like kinase 1) belongs to a class of serine/threonine kinases, and they have attracted increasing attention because of their critical roles in the regulation of mitosis and cytokinesis. Four mammalian Plk family members, *i.e.* Plk1, Plk2/SNK, Plk3/FNK/PRK, and Plk4/SAK, have been identified (1). Plk1 is the best characterized member of the human Plk family. It localizes to the centrosomes and kinetochores in late S or early G_2 and then translocates to the spindle pole and central spindle during mitosis and cytokinesis (1). Consistent with its intracellular distribution, Plk1 regulates multiple events during cell cycle progression, such as centrosome amplification and maturation, mitotic exit, mitotic spindle assembly, spindle pole maintenance, and cytokinesis (2–13). Plk1 can phosphorylate a number of proteins that are implicated in the regulation of cytokinesis, such as ECT2 (9, 14), NudC (5), ROCK2 (Rho-associated coiled-coil domain-containing protein kinase 2) (15), Cep55 (16), and Mklp2 (mitotic kinesin-like protein 2) (17).

Evidence has accumulated to suggest that the central spindle plays a critical role in signaling furrow ingression during cytokinesis (18, 19). Interaction between Plk1 and Mklp2 appears to be important for the localization of Plk1 to the central spindle. Depletion Mklp2 by RNAi[2] disrupts the localization of Plk1 at the central spindle, leading to a failure in furrow ingression and cytokinesis (17). Further studies demonstrate that Plk1 is responsible for recruiting ECT2 to the central spindle, where ECT2 locally activates the small GTPase protein RhoA at the cleavage furrow. In turn, RhoA induces myosin contractile ring assembly as well as furrow formation and ingression (9, 10, 14). In cells treated with the small molecule inhibitor for Plk1, ECT2 does not interact with MgcRacGAP (HsCyk-4) and fails to localize to the central spindle, suggesting that Plk1 inhibitor prevents the localization of ECT2 to the central spindle by interfering with ECT2-MgcRacGAP interaction (9). However, depletion of ECT2 does not completely abrogate equatorial RhoA activation during cytokinesis (20), suggesting that other GEFs may also contribute to RhoA activation at the cleavage furrow.

We reported previously that MyoGEF, a guanine nucleotide factor, localizes to the spindle pole and central spindle (21). In this study, we demonstrate that Plk1 can phosphorylate MyoGEF on Thr-574. Plk1 and MyoGEF colocalize to the spindle pole and central spindle. We further show that phosphorylation of MyoGEF by Plk1 not only promotes the recruitment of MyoGEF to the central spindle but also enhances MyoGEF activity toward RhoA. Therefore, our results strongly suggest that Plk1 can regulate MyoGEF activity and localization, contributing to the regulation of cytokinesis.

EXPERIMENTAL PROCEDURES

Plasmid Constructs—Myc-tagged MyoGEF and GFP-tagged MyoGEF were described previously (21). Six MyoGEF truncation mutants corresponding to amino acids 71–388, 71–565, 392–565, 392–780, 559–790, and 479–780 were cloned into

* This work was supported, in whole or in part, by National Institutes of Health Grants k22 HL071542 (to Q. W.) and P20 RR17708 and P20 RR15563. This work was also supported by a fund from the Terry C. Johnson Center for Basic Cancer Research (to Q. W.). This is contribution 08-296-J from the Kansas Agricultural Experiment Station (Manhattan, KS). The costs of publication of this article were defrayed in part by the payment of page charges. This article must therefore be hereby marked "*advertisement*" in accordance with 18 U.S.C. Section 1734 solely to indicate this fact.

[S] The on-line version of this article (available at http://www.jbc.org) contains supplemental Movie S1 and Fig. S1.

[1] To whom correspondence should be addressed: Dept. of Biochemistry, Kansas State University, 141 Chalmers Hall, Manhattan, KS 66506. Tel.: 785-532-6736; Fax: 785-532-7278; E-mail: weiq@ksu.edu.

[2] The abbreviations used are: RNAi, RNA interference; siRNA, small interfering RNA; GST, glutathione *S*-transferase; DAPI, 4′,6′-diamino-2-phenylindole; MOPS, 4-morpholinepropanesulfonic acid; GEF, guanine nucleotide exchange factor; WT, wild type; PBD, polo-box domain; GFP, green fluorescent protein.

pCMV-3Tag2B (Stratagene) and pGEX-5X-1 (GE Healthcare) expression vectors. MyoGEF mutants (T574A, T574E, T585A, and T620A) were generated by site-directed mutagenesis according to the manufacturer's instructions (Stratagene) and confirmed by DNA sequencing.

Cell Culture and Synchronization—HeLa cells were maintained in Dulbecco's modified Eagle's medium supplemented with 10% fetal bovine serum. Cell cycle synchronization was performed by double thymidine block. Briefly, the transfected HeLa cells were treated with 2 mM thymidine for 24 h, cultured in thymidine-free medium for 10 h, and then treated with 2 mM thymidine for 16 h, followed by "release" to progress through the cell cycle in thymidine-free medium for the indicated time periods. Transfection of plasmids or siRNA into HeLa cells were done by using Lipofectamine 2000 (Invitrogen) according to the manufacturer's instructions. For transfection with plasmids, the transfected cells were analyzed ~24 h after transfection. For transfection with siRNA or siRNA plus plasmids, the transfected cells were analyzed ~48–72 h after transfection. The siRNA sequence for human Plk1 is as follows: AAGGGCGGCTTTGCCAAGTGCTT (6). Plk1 siRNA was purchased from Dharmacon. Plk1 inhibitor GW 843682X was purchased from Tocris Biosciences.

Expression and Purification of GST Fusion Proteins—GST-fused MyoGEF polypeptides were expressed in a bacterial expression system. BL21 bacterial cells expressing GST-MyoGEF polypeptides were homogenized by sonication and lysed in phosphate-buffered saline containing 1% Triton X-100 for 1 h at 4 °C. The GST fusion proteins were purified by using glutathione-conjugated agarose beads, eluted with 100 mM Tris-HCl (pH 7.5), 5 mM glutathione, and dialyzed against 50 mM Tris-HCl (pH 7.5), 50 mM NaCl.

Immunoprecipitation—Immunoprecipitation and GST pull-down assays were carried out as described previously (21, 22). Briefly, transfected cells were lysed in radioimmune precipitation assay lysis buffer (50 mM Tris-HCl, pH 7.4, 150 mM NaCl, 1% Nonidet P-40, 2.5% sodium deoxycholate, 1 mM EDTA, 1 mM phenylmethylsulfonyl fluoride, 1 μg/ml aprotinin, 1 μg/ml leupeptin, 1 μg/ml pepstatin, 1 mM Na_3VO_4, 1 mM NaF) for 10 min on ice. Cell extracts were collected and precleared with protein A/G-agarose beads. The precleared lysate was incubated with agarose-conjugated anti-Myc antibody overnight at 4 °C. After washing three times with radioimmune precipitation assay lysis buffer, the bound proteins were eluted with SDS loading buffer.

Immunoblotting—Cell lysates or immunoprecipitates were separated by 7% SDS-PAGE gel, transferred to an Immobilon-P transfer membrane (Millipore), blocked in 5% nonfat milk, and incubated with primary antibodies as indicated. The following primary antibodies were used: mouse anti-Myc (9E10, 1:1000; Santa Cruz), mouse anti-Plk1 (1:1000; Invitrogen), rabbit anti-phosphohistone 3 (1:1000; Millipore), rabbit anti-phosphothreonine (1:500; Invitrogen), rabbit anti-GFP (1:1000; Santa Cruz), rabbit anti-β-tubulin (1:2000; Santa Cruz), and rabbit anti-MyoGEF (1:250) (21). The blots were washed and incubated with horseradish peroxide-conjugated secondary antibodies (1:5000; Santa Cruz) for 1 h at 23 °C. The blots were visualized by SuperSignal West Pico Luminol/Enhancer solution (Pierce).

Immunofluorescence Staining and Time Lapse Microscopy—HeLa cells grown on coverslips were fixed in methanol/acetone (1:1; for anti-MyoGEF) for 12 min at −20 °C or in 4% paraformaldehyde for 12 min at 23 °C. After blocking with 1% bovine serum albumin for 1 h at 23 °C, the transfected cells were incubated with primary antibodies as indicated for 3 h at 23 °C or overnight at 4 °C, followed by incubation with secondary antibodies for 40 min at 23 °C. The primary antibodies used for immunofluorescence were as follows: monoclonal anti-β-tubulin antibody (Sigma; 1:1000), rabbit polyclonal MyoGEF antibody (1:100), and mouse anti-Plk1 (1:100; Invitrogen). The secondary antibodies, rhodomine goat anti-mouse IgG (1:500) and rhodomine goat anti-rabbit IgG (1:500), were purchased from Invitrogen. The nuclei were visualized by DAPI (Sigma). The coverslips were mounted using a Prolong antifade kit (Invitrogen). The images were collected by using a Leica DMI 6000 B microscope (Leica) and were then processed by deconvolution.

For time lapse microscopy, the cells grown in coverglass chambers were transfected with plasmids or siRNA as indicated. The transfected cells were cultured in Leibovitz's L-15 medium (ATCC) supplemented with 10% fetal bovine serum. Images of the live transfected cells were taken every 20 s using a Leica DMI 6000 B microscope (Leica).

In Vitro Kinase Assays—For Plk1 *in vitro* kinase assay, 5 μg of purified GST-fused MyoGEF fragments were incubated with 0.5 μg of recombinant His-Plk1 (Cell Signaling) in kinase buffer (5 mM MOPS, pH 7.2, 2.5 mM β-glycerophosphate, 1 mM EGTA, 4 mM $MgCl_2$, 0.05 mM dithiothreitol, 250 μM ATP) and 1 μCi of [γ32]-ATP. For the Cdk1 kinase assay, 5 μg of GST-fused MyoGEF fragments were incubated with 0.5 μg of purified GST-fused recombinant Cdk1/cyclinB complex (Cell Signaling) in kinase buffer (25 mM Tris-HCl, pH 7.5, 10 mM $MgCl_2$, 5 mM β-glycerophosphate, 0.1 mM sodium vanadate, 2 mM dithiothreitol, 200 μM ATP) and 1 μCi of [γ-^{32}P]ATP. The reaction mixtures were incubated at 30 °C for 30 min in 50 μl and resolved on SDS-PAGE gels. The gels were dried and subjected to autoradiography.

Dephosphorylation—Myc-MyoGEF immunoprecipitates were washed twice with complete lysis buffer, twice with lysis buffer without phosphatase inhibitors, and finally once with the lambda phosphatase reaction buffer (50 mM Tris-HCl, pH 7.5, 0.1 mM EDTA, 5 mM dithiothreitol, 0.01% Brij35). The immunoprecipitates were incubated for 30 min at 30 °C in the presence or absence of 1 μl of lambda phosphatase (Biolabs), washed twice with lysis buffer containing phosphatase inhibitors to stop the reaction, and then used in a GEF exchange assay.

In Vitro Guanine Nucleotide Exchange Analysis—The GEF exchange assay was conducted using a fluorescence-based spectroscopic analysis, which measured the incorporation of a fluorescence analog of GTP, *N*-methylanthraniloyl (mant)-GTP onto small GTPase RhoA. Briefly, lysates from HeLa cells expressing Myc-MyoGEF or Myc-MyoGEFT574A or from HeLa cells transfected with Plk1 siRNA and a plasmid encoding Myc-MyoGEF were immunoprecipitated using anti-Myc antibody-conjugated agarose and washed four times with lysis

buffer. 10 μg of GST-tagged RhoA were equilibrated in exchange buffer containing 40 mM Tris-HCl, pH 7.5, 100 mM NaCl, 20 mM $MgCl_2$, 1 mM dithiothreitol, 100 μg/ml bovine serum albumin, and 400 nM mant-GTP (Invitrogen). After taking a few measurements of steady readings at 25 °C using a Perkin-Elmer Life Sciences Victor 3, the Myc-MyoGEF or IgG immunoprecipitates were added, and the relative fluorescence of mant-GTP (excitation λ, 360 nm; emission λ, 440 nm) was monitored.

Rhotekin Pull-down Assay—The Rhotekin pull-down assay was carried out as described previously (21).

RESULTS

Plk1 Phosphorylates MyoGEF on Thr-574—Evidence has shown that Plk1 plays a central role in regulating cytokinesis (9, 10, 14, 15, 23). Analysis of the MyoGEF amino acid sequence revealed that there are at least seven potential Plk1 phosphorylation sites. To determine whether Plk1 can phosphorylate MyoGEF, three GST-tagged MyoGEF fragments 71–388, 71–565, and 392–780 were used in an *in vitro* kinase assay with purified recombinant Plk1. Among these overlapping MyoGEF polypeptides, only GST-392–780 fragment was phosphorylated by Plk1 *in vitro* (Fig. 1*B*, *lane 8*), indicating that the Plk1 phosphorylation sites are located between amino acids 565 and 780 (Fig. 1, *A* and *B*). Further analysis of the MyoGEF amino acid sequence revealed that Plk1 could most likely phosphorylate MyoGEF on Thr-574 based on the Plk1 consensus phosphorylation site (24, 25). To confirm this prediction, we mutated Thr-574 to alanine in the 392–780 fragment and used it as a substrate for the Plk1 *in vitro* kinase assay. A point mutation of threonine 574 to alanine (T574A) abolished the phosphorylation of 392–780 fragment by Plk1in vitro (Fig. 1*B*, compare *lane 6* with *lane 8*). These results strongly suggest that Thr-574 can be phosphorylated by Plk1 *in vitro*.

To determine whether Plk1 could phosphorylate Thr-574 *in vivo*, we transfected plasmids encoding Myc-MyoGEF wild type (WT) or Myc-MyoGEF-T574A into HeLa cells. The immunoprecipitated Myc-MyoGEF-WT and Myc-MyoGEF-T574A were subjected to immunoblot analysis with an antibody specific for phosphorylated threonine (Thr(P)). Fig. 1*C* shows that Myc-MyoGEF-WT (Myc-WT) was threonine-phosphorylated (*lane 1*). In contrast, mutation of Thr-574 to alanine (T574A) dramatically decreased threonine phosphorylation (Fig. 1*C*, compare *lane 1* with *lane 2*). We also mutated two other potential threonine phosphorylation sites (Thr-585 and Thr-620) to alanines (Myc-T585A and Myc-T620A). The immunoprecipitated Myc-T585A and Myc-T620A were also subjected to immunoblot analysis with Thr(P) antibody. Mutation of Thr-585 and Thr-620 to alanines did not affect threonine phosphorylation of MyoGEF (Fig. 1*C*, compare *lanes 3* and *4* with *lane 1*). These results show that MyoGEF is phosphorylated on Thr-574 *in vivo*.

To determine whether the phosphorylation is sensitive to Plk1 depletion, we transfected HeLa cells with a plasmid encoding Myc-MyoGEF and control siRNA or Plk1 siRNA. 48 h after transfection, the transfected cells were subjected to immunoprecipitation with normal IgG or with anti-Myc antibody. The resulting immunoprecipitates were then subjected to immunoblot analysis with antibodies specific for Thr(P) and MyoGEF. As shown in Fig. 1*D*, depletion of Plk1 dramatically decreased threonine-phosphorylation of MyoGEF (compare *lane 2* with *lane 4* in the *upper panel*).

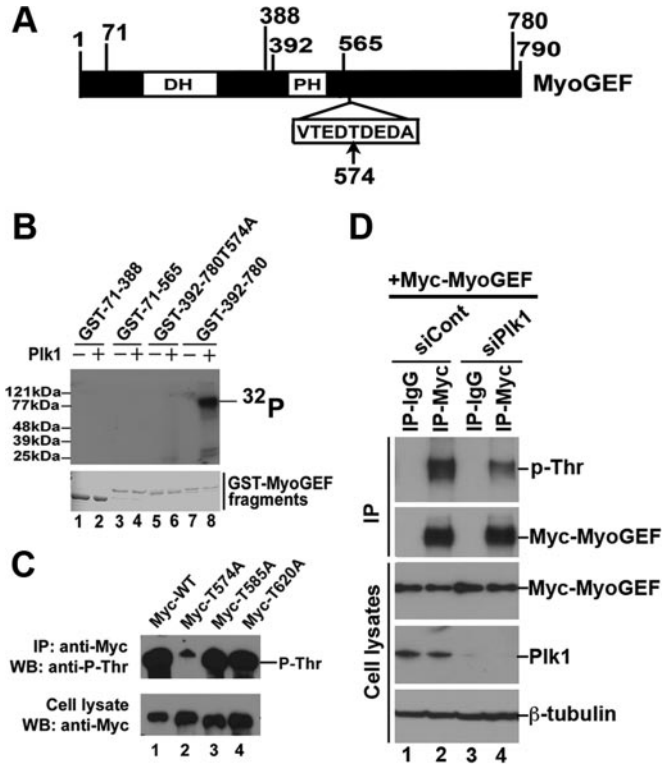

FIGURE 1. **Plk1 phosphorylates MyoGEF on Thr-574.** *A*, schematic diagram of MyoGEF. The *numbers* indicate the amino acids. *T574*, threonine 574. *DH*, Dbl homology domain. *PH*, pleckstrin homology domain. *B*, Plk1 phosphorylates MyoGEF *in vitro*. Four GST-tagged MyoGEF polypeptides were incubated with or without purified Plk1 in the presence of [γ-^{32}P]ATP. The proteins were resolved on SDS-PAGE gel and visualized by autoradiography (*upper panel*) or Coomassie Blue staining (*lower panel*). *C*, Plk1 phosphorylates MyoGEF *in vivo*. HeLa cells were transfected with plasmids encoding wild type full-length MyoGEF (Myc-WT) or mutated full-length MyoGEF (Myc-T574A, Myc-T585A, or Myc-T620A). Anti-Myc-conjugated agarose was used to precipitate Myc-tagged proteins from transfected cell lysates, followed by immunoblot analysis with anti-phosphothreonine antibody. *D*, threonine-phosphorylation of MyoGEF in transfected cells is sensitive to Plk1 depletion. HeLa cells were transfected with a plasmid encoding Myc-MyoGEF and control siRNA (*siCont*; *lanes 1* and *2*) or Plk1 siRNA (*siPlk1*; *lanes 3* and *4*). The unsynchronized transfected cells were subjected to immunoprecipitation with normal control IgG or anti-Myc antibody. *WB*, Western blot; *IP*, immunoprecipitation.

Thr-574 Is Specifically Phosphorylated in Mitosis—Plk1 is a mitotic kinase that mainly functions during mitosis and cytokinesis (9, 10, 14, 15, 23). MyoGEF localizes to the cleavage furrow and plays a role in regulating cytokinesis (21). One would expect that MyoGEF is likely to be phosphorylated by Plk1 specifically during mitosis and cytokinesis. To test this idea, we transfected HeLa cells with plasmids encoding Myc-MyoGEF-WT (Fig. 2*A*, *top two panels*) or Myc-MyoGEF-T574A (Fig. 2*A*, *middle two panels*). The transfected cells were synchronized at mitosis as described under "Experimental Procedures." Immunoblot analysis was carried out with an antibody specific for phosphohistone 3 to confirm that the transfected cells were enriched in mitosis at 10–14 h following release from double thymidine block (Fig. 2*A*, *bottom two panels*). The immunoprecipitated Myc-MyoGEF-WT or Myc-MyoGEF-

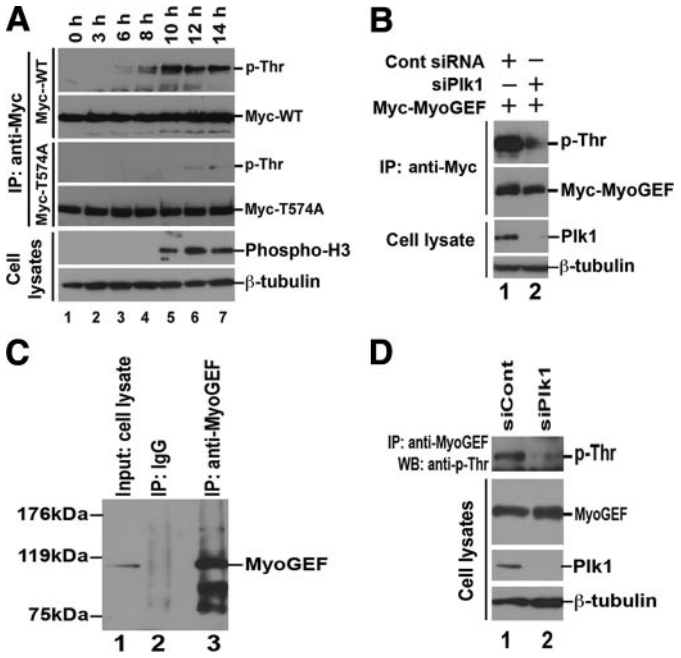

FIGURE 2. **MyoGEF is phosphorylated by Plk1 on Thr-574 in mitosis.** *A*, phosphorylation of MyoGEF in mitosis. HeLa cells expressing Myc-WT or Myc-T574A were synchronized at the G_1/S border by double-thymidine block and then released to progress through the cell cycle. Threonine phosphorylation of MyoGEF at different stages of the cell cycle (at 0–14 h release from double thymidine block) was assessed by immunoprecipitation with anti-Myc-conjugated agarose, followed by immunoblot analysis with phosphothreonine-specific (Thr(P)) antibody. *B*, Plk1 can phosphorylate MyoGEF *in vivo*. A plasmid encoding Myc-MyoGEF were cotransfected into HeLa cells with control siRNA (*lane 1*) or Pk1 siRNA (*siPlk1*; *lane 2*). The transfected cells were synchronized at the G_1/S border by double-thymidine block and then released for 12 h to progress to mitosis. Threonine phosphorylation of MyoGEF at mitosis was assessed as described in *A*. *C*, endogenous MyoGEF can be immunoprecipitated by an antibody specific for MyoGEF (compare *lane 2* with *lane 3*). U2OS cell lysate was subjected to immunoprecipitation with an antibody specific for MyoGEF, followed by immunoblot analysis with anti-MyoGEF antibody. *D*, threonine-phosphorylation of endogenous MyoGEF is sensitive to Plk1 depletion. U2OS cells were transfected with control siRNA (*siCont*; *lane 1*) or Plk1 siRNA (*siPLk1*; *lane 2*). The transfected cells were synchronized as described in *B*. The transfected cell lysates were subjected to immunoprecipitation with anti-Myc antibody, followed by immunoblot analysis with Thr(P) antibody. *WB*, Western blot; *IP*, immunoprecipitation.

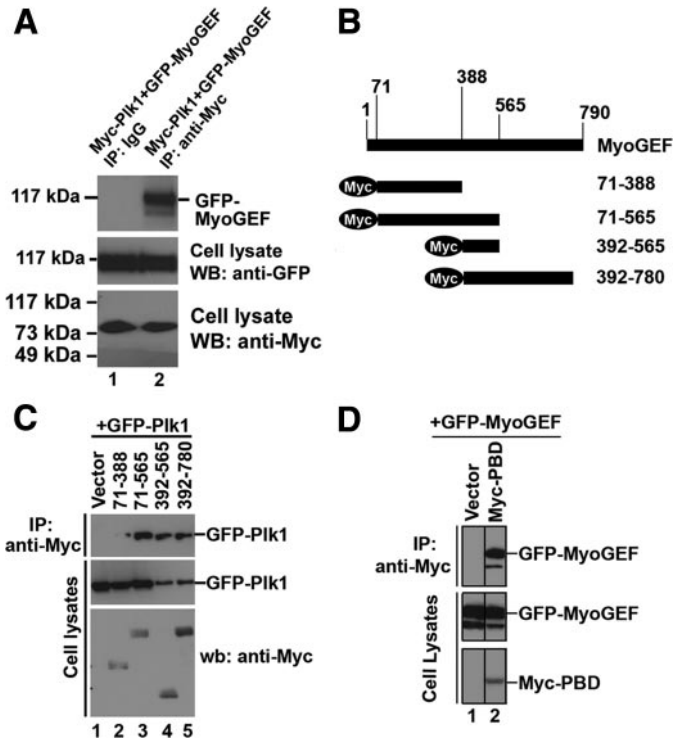

FIGURE 3. **Interaction between MyoGEF and Plk1.** *A*, HeLa cells were transfected with plasmids encoding Myc-Plk1 and GFP-MyoGEF. Anti-Myc-conjugated agarose was used to precipitate Myc-Plk1 from the transfected cell lysate, followed by immunoblotting with an antibody specific for GFP. *B*, schematic diagram of MyoGEF fragments. The numbers indicate the amino acids. *C*, a plasmid encoding GFP-Plk1 was cotransfected into HeLa cells with empty vector or plasmids encoding Myc-tagged MyoGEF fragments (71–388, 71–565, 392–565, or 392–780). Anti-Myc-conjugated agarose was used to precipitate Myc-tagged MyoGEF fragments from the transfected cell lysate, followed by immunoblotting with an antibody specific for GFP. *D*, a plasmid encoding GFP-MyoGEF was cotransfected into HeLa cells with empty vector or a plasmid encoding Myc-PBD. Anti-Myc-conjugated agarose was used to precipitate Myc-PBD from the transfected cell lysate, followed by immunoblotting with an antibody specific for GFP. *wb*, Western blot; *IP*, immunoprecipitation.

T574A was subjected to immunoblot analysis with Thr(P) antibody. As shown in Fig. 2*A*, Myc-WT was mainly phosphorylated at ~10–14 h following release from double thymidine block (*lanes 5–7*, *top two panels*). In contrast, replacement of threonine 574 with a nonphosphorylatable alanine dramatically decreased *in vivo* phosphorylation of transfected MyoGEF (Fig. 2*A*, *middle two panels*). These finding suggests that MyoGEF is preferentially phosphorylated during mitosis.

To further confirm that MyoGEF is phosphorylated by Plk1, we transfected HeLa cells with a plasmid encoding Myc-MyoGEF and control siRNA or Plk1 siRNA. The transfected cells were subjected to double thymidine block as described under "Experimental Procedures." Because MyoGEF was phosphorylated at 12 h following release from thymidine block (Fig. 2*A*), we selected this time point to assess whether treatment with Plk1 siRNA had an effect on threonine phosphorylation of MyoGEF. Approximately 62 h after siRNA transfection (at 12 h following release from thymidine block), Myc-MyoGEF was immunoprecipitated with anti-Myc-conjugated agarose and subjected to immunoblot analysis with phosphothreonine antibody. As shown in Fig. 2*B*, cotransfection with Plk1 siRNA decreased threonine phosphorylation of Myc-MyoGEF (compare *lane 1* with *lane 2* in the *upper panel*). These results suggest that Plk1 can mediate threonine-phosphorylation of MyoGEF *in vivo*.

To determine whether endogenous MyoGEF could be phosphorylated by Plk1, we transfected U2OS cells with control siRNA or Plk1 siRNA. The transfected cells were collected at mitosis as described under "Experimental Procedures." As shown in Fig. 2*D*, depletion of Plk1 by RNAi dramatically decreased threonine phosphorylation of endogenous MyoGEF (compare *lane 1* with *lane 2* in the *top panel*). Fig. 2*C* shows that MyoGEF antibody could immunoprecipitate endogenous MyoGEF from U2OS cells. We selected U2OS cells for this experiment, because this cell line expresses a higher level of MyoGEF than HeLa cells (21).

Consistent with the above observations, Myc-Plk1 was coimmunoprecipitated with GFP-MyoGEF from transfected HeLa cells (Fig. 3*A*, compare *lane 1* with *lane 2* in the top panel). We also constructed expressing plasmids that contain several overlapping MyoGEF fragments (Fig. 3*B*). These plasmids were cotransfected into HeLa cells with a plasmid encoding GFP-

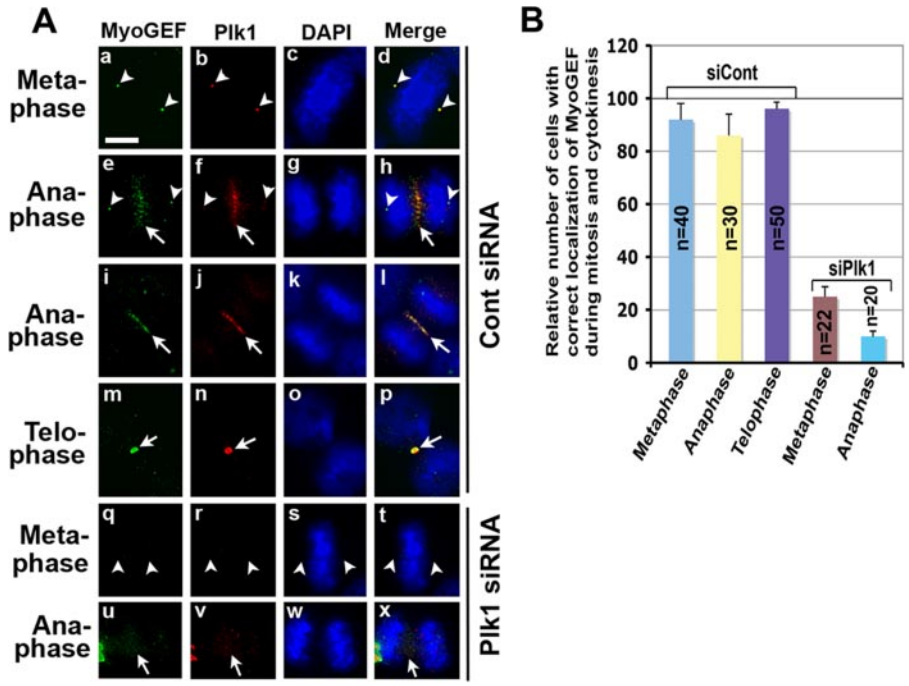

FIGURE 4. **Plk1 is required for MyoGEF localization to the spindle pole and central spindle.** *A*, HeLa cells grown on coverslips were transfected with control siRNA (*panels a–p*) or Plk1 siRNA (*panels q–x*). 48 h following transfection, the transfected cells were fixed in methanol/acetone and subjected to immunofluorescence with antibodies specific for Plk1 (*red*) or MyoGEF (*green*). The nuclei were stained with DAPI (*blue*). The *arrowheads* indicate the spindle poles. The *arrows* indicate the central spindles or midbodies. *Bar*, 20 μm. *B*, quantification of results in *A*. The number (*n*) represents the mitotic cells examined.

Plk1. Coimmunoprecipitation experiment showed that GFP-Plk1 could interact with MyoGEF fragments 71–565, 392–565, and 392–780, but not 71–388 (Fig. 3*C*), indicating that amino acids 388–565 of MyoGEF can interact with Plk1. Plk1 interacts with its substrates through the polo-box domain (PBD) (15, 24, 26–28). Therefore, we asked whether PBD could bind MyoGEF. As shown in Fig. 3*D*, a plasmid encoding GFP-MyoGEF was cotransfected into HeLa cells with empty plasmid (*lane 1*) or a plasmid encoding Myc-PBD (*lane 2*). PBD was coimmunoprecipitated with GFP-MyoGEF (Fig. 3*D*, compare *lane 1* with *lanes 2* in the *top panel*), suggesting that PBD could bind MyoGEF.

Depletion of Endogenous Plk1 Interferes with the Localization of MyoGEF to the Central Spindle—Consistent with its critical role in regulating cytokinesis, Plk1 localizes to the spindle pole and central spindle (1). Plk1 phosphorylated MyoGEF on Thr-574 during mitosis and cytokinesis (Fig. 2). We have also shown previously that MyoGEF localizes to the spindle pole and central spindle (21). Therefore, we asked whether MyoGEF colocalizes with Plk1 during mitosis and cytokinesis. HeLa cells were fixed with methanol/acetone and stained with antibodies specific for MyoGEF and Plk1. As shown in Fig. 4, MyoGEF colocalized with Plk1 to the centrosome/spindle pole in metaphase (*arrowheads* in *panels a–d*) and then concentrated at the central spindle in anaphase (*arrows* in *panels e–l*) and midbody in telophase (*arrows* in *panels m–p*). Plk1 and MyoGEF also colocalized to the spindle pole in anaphase (*arrowheads* in *panels e–h*), but the signals were weaker than those in metaphase (*arrowheads* in *panels a–h*; compare *panels a–d* with *panels e–h*).

We further asked whether Plk1 is required for the localization of MyoGEF to the spindle pole and central spindle. It has been shown that most of the cells depleted of Plk1 by RNAi were arrested in mitosis. However, ~15% of Plk1-depleted cells can advance to anaphase, although they do not complete cytokinesis (6). HeLa cells were transfected with control or Plk1 siRNA. 48 h following transfection, the transfected HeLa cells were fixed and stained with antibodies specific for Plk1 or MyoGEF. In HeLa cells depleted of Plk1, MyoGEF was not concentrated at the spindle pole and central spindle (Fig. 4*A*, *panels q–x*). Approximately 20–50 cells at each stage of mitosis and cytokinesis were analyzed, and the results were quantified in Fig. 4*B*.

Disruption of Endogenous MyoGEF Localization by Plk1 Inhibitor—To further confirm that Plk1 activity is required for the localization of MyoGEF to the central spindle, we also examined whether Plk1 inhibitor GW 843682X affected MyoGEF localization during cytokinesis. HeLa cells were treated with GW 843682X for ~40 min and then subjected to immunofluorescence with anti-MyoGEF antibody. As shown in Fig. 5, Plk1 inhibitor interfered with the localization of endogenous MyoGEF at the central spindle (compare *panels a* and *d* with *panels e* and *h*). These results confirmed that Plk1 plays a role in regulating MyoGEF localization during cytokinesis.

Localization of GFP-MyoGEF Mutants during Cytokinesis—To further characterize the role of Plk1-mediated phosphorylation in regulating MyoGEF localization, we examined the localization of GFP-tagged wild type and mutants of MyoGEF during cytokinesis. We transfected HeLa cells with plasmids encoding GFP-MyoGEF-wt, GFP-MyoGEF-T574A, or GFP-MyoGEF-T574E. The transfected cells were processed for immunofluorescence with an antibody specific for β-tubulin. As shown in Fig. 6*A*, GFP-MyoGEF-wt (GFP-WT; *panels a–d*) and GFP-MyoGEF-T574E (GFP-T574E; *panels i–l*) show similar localization during cytokinesis, *i.e.* they both localize to the central spindle (*arrows*). Although GFP-MyoGEF-T574A (GFP-T574A) also localized to the central spindle, it shows a more diffuse distribution at the central spindle (Fig. 6*A*, *arrows* in *panels e* and *h*), indicating that phosphorylation at Thr-574 can promote the localization of MyoGEF to the central spindle. These findings are consistent with results from both RNAi and Plk1 inhibitor experiments (Figs. 4 and 5).

We then asked whether the small molecule inhibitor of Plk1, GW 843682X, interfered with the localization GFP-MyoGEF during cytokinesis. As shown in Fig. 6*B*, treatment with Plk1

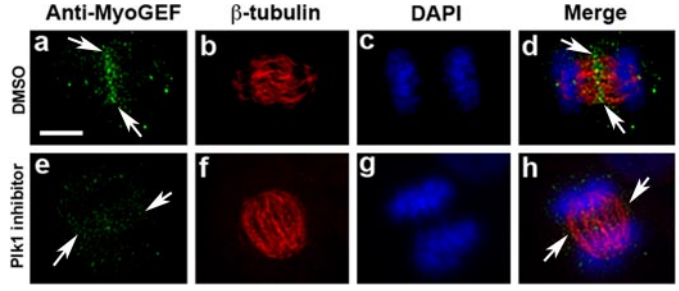

FIGURE 5. **Localization of endogenous MyoGEF at the central spindle is sensitive to Plk1 activity.** HeLa cells were cultured in the presence of Plk1 inhibitor for 30–40 min, fixed in methanol/acetone, and processed for immunofluorescence with antibodies specific for β-tubulin (*red*) and MyoGEF (*green*). The nuclei were stained with DAPI (*blue*). *Bar*, 20 μm. *DMSO*, dimethyl sulfoxide.

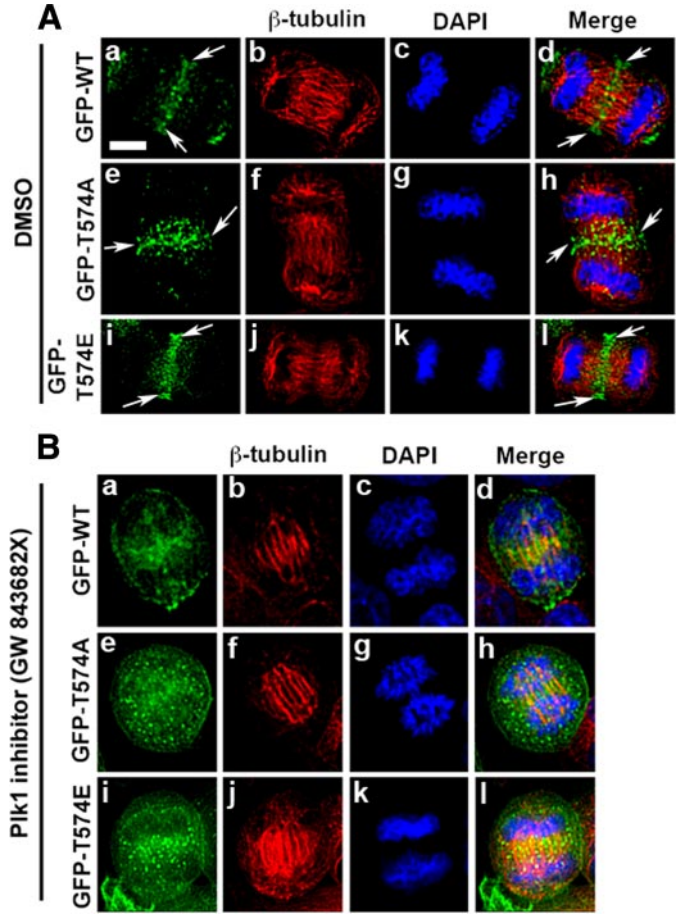

FIGURE 6. **Localization of GFP-tagged MyoGEF at the central spindle is sensitive to Plk1 activity.** *A*, localization of GFP-tagged MyoGEF at the central spindle. HeLa cell were transfected with plasmids encoding GFP-MyoGEF-wt (GFP-WT; *panels a–d*), GFP-MyoGEF-T574A (GFP-T574A; *panels e–h*), or GFP-MyoGEF-T574E (GFP-T574E; *panels i–l*). Arrows indicate the central spindle. *B*, the transfected cells in *A* were cultured in the presence of Plk1 inhibitor GW 843682X at 1 μM for 30–40 min (41). The treated cells were fixed in 4% paraformaldehyde and processed for immunofluorescence with an antibody specific for β-tubulin (*red*). The nuclei were stained with DAPI (*blue*). *Bar*, 20 μm. *DMSO*, dimethyl sulfoxide.

inhibitor disrupted the localization of GFP-MyoGEF-wt (GFP-WT; *panels a–d*), GFP-MyoGEF-T574A (GFP-T574A; *panels e–h*), and GFP-MyoGEF-T574E (GFP-T574E; *panels i–l*) to the central spindle. These results further demonstrate a critical role for Plk1 in regulating MyoGEF localization during cytokinesis.

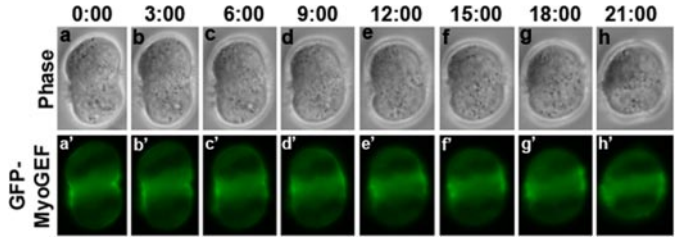

FIGURE 7. **Exogenous expression of GFP-MyoGEF results in furrow regression.** HeLa cells were transfected with a plasmid encoding GFP-MyoGEF. 24 h after transfection, the live transfected cells were monitored using a Leica DMI 6000 B microscope (Leica). The *number* indicates the time elapsed.

Exogenous Expression of GFP-MyoGEF Caused Furrow Regression—We previously showed that GFP-MyoGEF localizes to the central spindle and cleavage furrow in fixed transfected cells (21). To further understand the dynamic localization of GFP-MyoGEF, we used time lapse microscopy to monitor the localization of GFP-MyoGEF in the transfected cells during cytokinesis. We found that ~60% ($n = 38/60$) of the cells exogenously expressing GFP-MyoGEF showed furrow regression and failed to complete cytokinesis (Fig. 7 and supplemental Movie S1), suggesting that overexpression of MyoGEF could also lead to defects in cytokinesis. Exogenous expression of GFP-MyoGEF-T574A and GFP-MyoGEF-T574E also led to furrow regression (data not shown). It has also been reported that exogenous expression of ECT2 can cause failure in cytokinesis (14).

Phosphorylation of MyoGEF on Thr-574 Enhanced Its Activity toward RhoA—We previously reported that RNAi-mediated depletion of MyoGEF led to a decrease in RhoA activity (21). To determine whether Thr-574 phosphorylation has an impact on MyoGEF activity toward RhoA, we used a fluorescent based biochemical GEF exchange assay to measure the incorporation of a fluorescence analog of GTP, *N*-methylanthraniloyl (mant)-GTP, onto the small GTPase RhoA. HeLa cells were transfected with a plasmid encoding Myc-MyoGEF-WT. The transfected cells were collected at 12 h following the second thymidine block. Myc-MyoGEF-WT was immunoprecipitated with anti-Myc antibody. The immunoprecipitates were treated with or without lambda phosphatase and then used in the GEF exchange assay. As shown in Fig. 8*A*, RhoA activity was dramatically increased in the presence of the Myc-MyoGEF-WT. In contrast, treatment of Myc-MyoGEF immunoprecipitate with phosphatase dramatically reduced MyoGEF activity toward RhoA (Fig. 8*A*), indicating that phosphorylation is important for MyoGEF-mediated activation of RhoA.

To confirm that Plk1-mediated phosphorylation of MyoGEF could directly enhance RhoA activation, HeLa cells were transfected with a plasmid encoding Myc-MyoGEF-WT and Plk1 siRNA or with a plasmid encoding Myc-MyoGEF-T574A. At 12 h following the second double thymidine block, the transfected cell lysates were immunoprecipitated with agarose-conjugated anti-Myc antibody and the immunoprecipitates were used in the *in vitro* GTPase assay. Fig. 8*A* shows that depletion of Plk1 by RNAi resulted in a decrease in MyoGEF-mediated RhoA activation. In addition, mutation of Thr-574 to alanine also reduced MyoGEF activity toward RhoA (Fig. 8*A*). Immunoblot analysis with anti-Myc antibody was carried to confirm

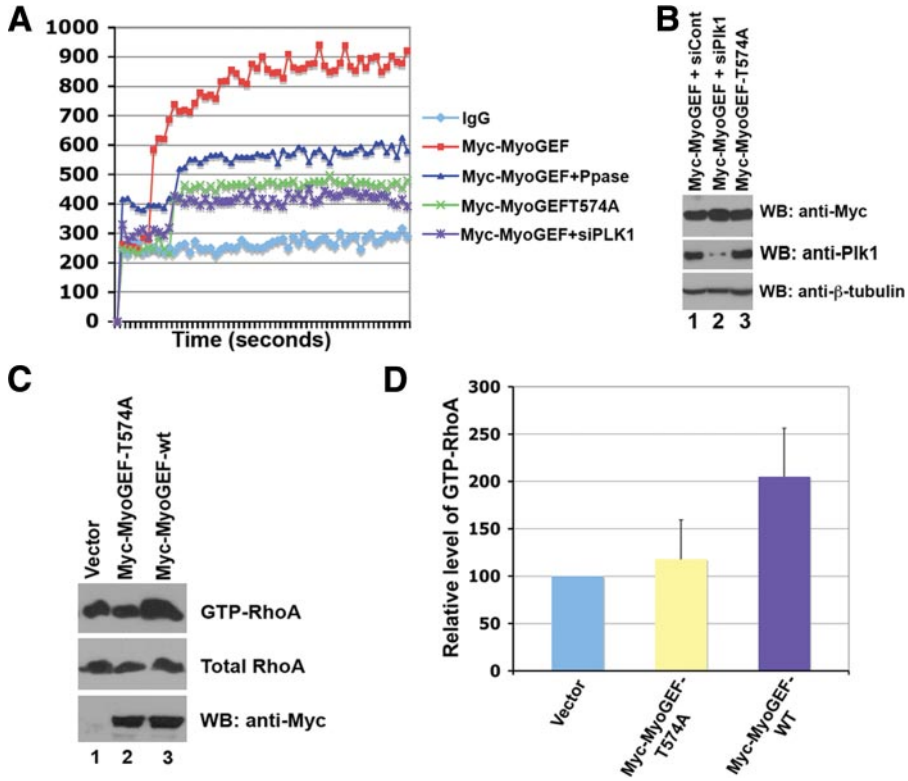

FIGURE 8. **Phosphorylation on Thr-574 increases MyoGEF activity toward RhoA.** *A*, HeLa cells were transfected with plasmids encoding Myc-MyoGEF-WT or Myc-MyoGEF-T574A or with a plasmid encoding Myc-MyoGEF plus Plk1 siRNA (*siPlk1*). Myc-MyoGEF-WT and Myc-MyoGEF-T574A were immunoprecipitated with anti-Myc-conjugated agarose. The immunoprecipitates were incubated with mant-GTP and purified GST-tagged RhoA, and the rate of nucleotide incorporation was measured over time. IgG immunoprecipitates were used as control (IgG). The Myc-MyoGEF-WT immunoprecipitates were treated with buffer (Myc-MyoGEF) or with λ-phosphatase (*Myc-MyoGEF+Ppase*) as described under "Experimental Procedures." The Myc-MyoGEF-T574A and Myc-MyoGEF+siPlk1 immunoprecipitates were treated with buffer (Myc-MyoGEFT574A and Myc-MyoGEF+siPlk1). *B*, immunoblot analysis with anti-Myc and anti-Plk1 antibodies shows the expression of Myc-tagged proteins used in *A* as well as the efficiency of Plk1 knockdown by RNAi. *C*, *in vivo* activity of Myc-tagged MyoGEF in transfected cells. HeLa cells were transfected with an empty plasmid (*Vector*) or plasmids encoding Myc-MyoGEF-T574A (*lane 2*) or Myc-MyoGEF-wt (*lane 3*). The transfected cells were synchronized at mitosis as described under "Experimental Procedures," and were then subjected to the rhotekin pull-down assay. Three independent experiments were done, and one of the blots was shown. *D*, quantification of results from *C*. The immunoblot images were quantified using the National Institutes of Health Image program. *WB*, Western blotting.

that the constructs used in Fig. 8*A* were expressed at similar levels (Fig. 8*B*). These results show that phosphorylation of Thr-574 in MyoGEF may play an important role in regulating MyoGEF activity toward RhoA.

To examine whether phosphorylation at Thr-574 plays a role in RhoA activation *in vivo*, we transfected HeLa cells with an empty vector or plasmids encoding Myc-MyoGEF-wt or Myc-MyoGEF-T574A. The transfected cells were enriched at mitosis and then subjected to the rhotekin pull-down assay described under "Experimental Procedures." As shown in Fig. 8 (*C* and *D*), exogenous expression of Myc-MyoGEF-wt, but not Myc-MyoGEF-T574A, greatly increased the level of GTP-RhoA. This result indicated that phosphorylation at Thr-574 may enhance MyoGEF activity toward RhoA.

DISCUSSION

In this study, we have demonstrated that Plk1 can phosphorylate MyoGEF on Thr-574, thereby contributing to the recruitment of MyoGEF to the central spindle as well as enhancing MyoGEF activity toward RhoA. We also show that Plk1 and MyoGEF colocalize at the spindle pole, central spindle, and midbody during mitosis and cytokinesis. RNAi-mediated depletion of Plk1 not only interferes with the localization of MyoGEF at the spindle pole and central spindle but also decreases MyoGEF activity toward RhoA in transfected HeLa cells. Our results strongly suggest that Plk1 regulates MyoGEF activity and localization during cytokinesis.

Plk1 is a key regulator of mitosis and cytokinesis (1). Our results show that MyoGEF is phosphorylated on Thr-574 in transfected HeLa cells during mitosis and cytokinesis (Figs. 1 and 2). *In vitro* kinase assay shows that Plk1 can phosphorylate a wild type MyoGEF fragment 392–780, but not the MyoGEF fragment with a point mutation of Thr-574 to alanine (T574A) (Fig. 1). Depletion of Plk1 by RNAi decreases threonine phosphorylation of MyoGEF (Fig. 2). These results strongly suggest that Plk1 can phosphorylate MyoGEF on Thr-574. We previously showed that MyoGEF is required for cytokinesis (21). Time lapse microscopy also demonstrates that depletion of MyoGEF results in furrow regression and metaphase arrest.[3] In this study, we have shown that Plk1 is required for the localization of MyoGEF to the spindle pole and central spindle. Thus, our results suggest that phosphorylation of MyoGEF by Plk1 plays a role in the regulation of cytokinesis. On the other hand, it has been demonstrated that Plk1 regulates furrow formation and ingression by phosphorylating ECT2 and recruiting it to the central spindle (9, 10). Consistently, a number of studies also show that ECT2 localizes to the central spindle and is responsible for the activation of RhoA at the cleavage furrow (14, 29–34). Although it is unclear at present how ECT2 and MyoGEF cooperate to regulate cytokinesis, our unpublished data[4] suggest that MyoGEF can interact with ECT2 and that depletion of MyoGEF interferes with ECT2 localization at the central spindle. In addition, depletion of either ECT2 or MyoGEF interferes with RhoA activation at the cleavage furrow (30, 33).[3] These results strongly suggest that ECT2 and MyoGEF may coordinate the regulation of cytokinesis.

Results from experiments with both Plk1 siRNA and Plk1 inhibitor strongly suggest that Plk1 plays a critical role in regu-

[3] M. Asiedu, D. Wu, F. Matsumura, and Q. Wei, submitted for publication.
[4] M. Asiedu, D. Wu, F. Matsumura, and Q. Wei, unpublished data.

lating MyoGEF localization at the central spindle (Figs. 4–6). Our results also indicated that Thr-574 is most likely the major phosphorylation site on MyoGEF by Plk1 (Figs. 1 and 2). However, mutation of Thr-574 to alanine did not completely disrupt MyoGEF localization at the central spindle (Fig. 6*A*). One possibility is that MyoGEF can form a dimer/oligomer. Indeed, formation of a dimer/oligomer can be a way to regulate the activity of GEFs (35–37). Coimmunoprecipitation experiments show that Myc-MyoGEF-WT can be coimmunoprecipitated with GFP-MyoGEF-T574A from transfected HeLa cell lysates.[4] Therefore, GFP-MyoGEF-T574A may localize to the central spindle by forming a dimer/oligomer with endogenous MyoGEF. Another possibility is that GFP-MyoGEF-T574A may localize to the central spindle by interacting with ECT2, because our unpublished data[4] suggest that MyoGEF can form a complex with ECT2. Consistent with these speculations, treatment with Plk1 inhibitor, which disrupts the localization of both endogenous MyoGEF and ECT2 localization at the central spindle (9, 10) (Fig. 5), interferes with the localization of GFP-tagged wild type and mutant MyoGEF (Fig. 6*B*).

We also noticed that GFP-MyoGEF did not localize to the spindle pole. This is most likely due to the presence of GFP tag. However, localization of endogenous MyoGEF at the spindle pole is not likely an artifact. First, depletion of MyoGEF by RNAi can decrease the staining at the spindle pole with MyoGEF antibody.[3] Second, absorption of MyoGEF antiserum with MyoGEF full-length protein can completely abrogate the spindle pole staining (supplemental Fig. S1).

Plk1 binds its substrates by interacting with a docking site (S-S*-P or S-T*-P) that is phosphorylated by priming kinases, such as CDK1 (1, 24, 25, 38, 39). Analysis of the MyoGEF sequence revealed that there are two potential Plk1 docking sites in MyoGEF, *i.e.* Thr-544 (S-*T544-P) and Ser-697 (S-*S697-P). Indeed, the *in vitro* kinase assay showed that Cdk1/cyclin B could phosphorylate MyoGEF (data not shown). However, mutations of Thr-544 or Ser-697 to alanines did not substantially change Cdk1 phosphorylation of MyoGEF fragments (data not shown), suggesting that Thr-544 and Ser-697 are not likely the major sites for Cdk1 in MyoGEF. Therefore, the priming kinase for Plk1-MyoGEF interaction remains to be determined.

Although ECT2 has been considered as the major GEF that is responsible for equatorial RhoA activation at the cleavage furrow (14, 29–34), evidence is accumulating that other proteins also contribute to equatorial RhoA activation. The armadillo protein p0071 localizes to the midbody and forms a complex with RhoA and ECT2. Full RhoA activation at the cleavage furrow requires both ECT2 and p007 (40). GEF-H1, a GEF that localizes to spindle apparatus and midbody, is critical for RhoA activation at late stages of cytokinesis (20). Immunofluorescence and coimmunoprecipitation experiments show that Plk1 can physically interact with RhoA at the midbody during cytokinesis (23), although it is not clear whether Plk1 can directly modulate RhoA activity at the cleavage furrow. Plk1 also phosphorylates ROCK2, a RhoA downstream effector, and synergistically acts with RhoA to enhance ROCK2 kinase activity (15). Our results show that activation of RhoA by MyoGEF is regulated by Plk1 phosphorylation (Fig. 8), suggesting that MyoGEF also contributes to RhoA activation during cytokinesis. Therefore, multiple pathways may contribute to equatorial RhoA activation to ensure robust cytokinesis in different cells under different conditions.

Acknowledgments—We thank Dr. Robert S. Adelstein and Dr. Mary Anne Conti for critical reading and comments on the manuscript. We also thank Dr. Keith Burridge for providing plasmid pGEX-RBD.

REFERENCES

1. Barr, F. A., Sillje, H. H., and Nigg, E. A. (2004) *Nat. Rev. Mol. Cell. Biol.* **5,** 429–440
2. Sumara, I., Gimenez-Abian, J. F., Gerlich, D., Hirota, T., Kraft, C., de la Torre, C., Ellenberg, J., and Peters, J. M. (2004) *Curr. Biol.* **14,** 1712–1722
3. van Vugt, M. A., van de Weerdt, B. C., Vader, G., Janssen, H., Calafat, J., Klompmaker, R., Wolthuis, R. M., and Medema, R. H. (2004) *J. Biol. Chem.* **279,** 36841–36854
4. Lindon, C., and Pines, J. (2004) *J. Cell Biol.* **164,** 233–241
5. Zhou, T., Aumais, J. P., Liu, X., Yu-Lee, L. Y., and Erikson, R. L. (2003) *Dev. Cell* **5,** 127–138
6. Liu, X., and Erikson, R. L. (2002) *Proc. Natl. Acad. Sci. U. S. A.* **99,** 8672–8676
7. Seong, Y. S., Kamijo, K., Lee, J. S., Fernandez, E., Kuriyama, R., Miki, T., and Lee, K. S. (2002) *J. Biol. Chem.* **277,** 32282–32293
8. Lane, H. A., and Nigg, E. A. (1996) *J. Cell Biol.* **135,** 1701–1713
9. Petronczki, M., Glotzer, M., Kraut, N., and Peters, J. M. (2007) *Dev. Cell* **12,** 713–725
10. Burkard, M. E., Randall, C. L., Larochelle, S., Zhang, C., Shokat, K. M., Fisher, R. P., and Jallepalli, P. V. (2007) *Proc. Natl. Acad. Sci. U. S. A.* **104,** 4383–4388
11. McInnes, C., Mazumdar, A., Mezna, M., Meades, C., Midgley, C., Scaerou, F., Carpenter, L., Mackenzie, M., Taylor, P., Walkinshaw, M., Fischer, P. M., and Glover, D. (2006) *Nat. Chem. Biol.* **2,** 608–617
12. Lenart, P., Petronczki, M., Steegmaier, M., Di Fiore, B., Lipp, J. J., Hoffmann, M., Rettig, W. J., Kraut, N., and Peters, J. M. (2007) *Curr. Biol.* **17,** 304–315
13. Yamashiro, S., Yamakita, Y., Totsukawa, G., Goto, H., Kaibuchi, K., Ito, M., Hartshorne, D. J., and Matsumura, F. (2008) *Dev. Cell* **14,** 787–797
14. Niiya, F., Tatsumoto, T., Lee, K. S., and Miki, T. (2006) *Oncogene* **25,** 827–837
15. Lowery, D. M., Clauser, K. R., Hjerrild, M., Lim, D., Alexander, J., Kishi, K., Ong, S. E., Gammeltoft, S., Carr, S. A., and Yaffe, M. B. (2007) *EMBO J.* **26,** 2262–2273
16. Fabbro, M., Zhou, B. B., Takahashi, M., Sarcevic, B., Lal, P., Graham, M. E., Gabrielli, B. G., Robinson, P. J., Nigg, E. A., Ono, Y., and Khanna, K. K. (2005) *Dev. Cell* **9,** 477–488
17. Neef, R., Preisinger, C., Sutcliffe, J., Kopajtich, R., Nigg, E. A., Mayer, T. U., and Barr, F. A. (2003) *J. Cell Biol.* **162,** 863–875
18. Cao, L. G., and Wang, Y. L. (1996) *Mol. Biol. Cell* **7,** 225–232
19. Wheatley, S. P., and Wang, Y. (1996) *J. Cell Biol.* **135,** 981–989
20. Birkenfeld, J., Nalbant, P., Bohl, B. P., Pertz, O., Hahn, K. M., and Bokoch, G. M. (2007) *Dev. Cell* **12,** 699–712
21. Wu, D., Asiedu, M., Adelstein, R. S., and Wei, Q. (2006) *Cell Cycle* **5,** 1234–1239
22. Wei, Q. (2005) *J. Biol. Chem.* **280,** 37790–37797
23. Dai, B. N., Yang, Y., Chau, Z., and Jhanwar-Uniyal, M. (2007) *Cell Prolif.* **40,** 550–557
24. Elia, A. E., Cantley, L. C., and Yaffe, M. B. (2003) *Science* **299,** 1228–1231
25. Elia, A. E., Rellos, P., Haire, L. F., Chao, J. W., Ivins, F. J., Hoepker, K., Mohammad, D., Cantley, L. C., Smerdon, S. J., and Yaffe, M. B. (2003) *Cell* **115,** 83–95
26. Cheng, K. Y., Lowe, E. D., Sinclair, J., Nigg, E. A., and Johnson, L. N. (2003) *EMBO J.* **22,** 5757–5768
27. Song, S., Grenfell, T. Z., Garfield, S., Erikson, R. L., and Lee, K. S. (2000) *Mol. Cell. Biol.* **20,** 286–298

28. Reynolds, N., and Ohkura, H. (2003) *J. Cell Sci.* **116,** 1377–1387
29. Nishimura, Y., and Yonemura, S. (2006) *J. Cell Sci.* **119,** 104–114
30. Kamijo, K., Ohara, N., Abe, M., Uchimura, T., Hosoya, H., Lee, J. S., and Miki, T. (2006) *Mol. Biol. Cell* **17,** 43–55
31. Chalamalasetty, R. B., Hummer, S., Nigg, E. A., and Sillje, H. H. (2006) *J. Cell Sci.* **119,** 3008–3019
32. Zhao, W. M., and Fang, G. (2005) *Proc. Natl. Acad. Sci. U. S. A.* **102,** 13158–13163
33. Yuce, O., Piekny, A., and Glotzer, M. (2005) *J. Cell Biol.* **170,** 571–582
34. Kim, J. E., Billadeau, D. D., and Chen, J. (2005) *J. Biol. Chem.* **280,** 5733–5739
35. Schmidt, A., and Hall, A. (2002) *Genes Dev.* **16,** 1587–1609
36. Zhu, K., Debreceni, B., Bi, F., and Zheng, Y. (2001) *Mol. Cell. Biol.* **21,** 425–437
37. Chikumi, H., Barac, A., Behbahani, B., Gao, Y., Teramoto, H., Zheng, Y., and Gutkind, J. S. (2004) *Oncogene* **23,** 233–240
38. Lowery, D. M., Mohammad, D. H., Elia, A. E., and Yaffe, M. B. (2004) *Cell Cycle* **3,** 128–131
39. Neef, R., Gruneberg, U., Kopajtich, R., Li, X., Nigg, E. A., Sillje, H., and Barr, F. A. (2007) *Nat. Cell Biol.* **9,** 436–444
40. Wolf, A., Keil, R., Gotzl, O., Mun, A., Schwarze, K., Lederer, M., Huttelmaier, S., and Hatzfeld, M. (2006) *Nat. Cell Biol.* **8,** 1432–1440
41. Lansing, T. J., McConnell, R. T., Duckett, D. R., Spehar, G. M., Knick, V. B., Hassler, D. F., Noro, N., Furuta, M., Emmitte, K. A., Gilmer, T. M., Mook, R. A., Jr., and Cheung, M. (2007) *Mol. Cancer Ther.* **6,** 450–459